Available online at www.qu.edu.iq/journalcm
JOURNAL OF AL-QADISIYAH FOR COMPUTER SCIENCE AND MATHEMATICS
ISSN:2521-3504(online) ISSN:2074-0204(print)

Influence of Temperature on The Concentration and thus on the MHD Oscillatory Flow of a Tangent Hyperbolic Fluid Through a Regular Permeable Channel

***Iman S. Salih Al-Shammari*[a], *Dheia G. Salih Al-Khafajy*[b,*]**

[a]*Department of Mathematics, College of Science, University of Al-Qadisiyah, Diwaniya, Iraq.Email: eamansad12344@gmail.com*

[b]*Department of Mathematics, College of Science, University of Al-Qadisiyah, Diwaniya, Iraq.Email: dheia.salih@qu.edu.iq, dr.dheia.g.salih@gmail.com*

ARTICLE INFO

Article history:
Received: 14 /5/2024
Revised form: 12 /6/2024
Accepted : 23 /6/2024
Available online: 30 /6/2024

Keywords: Tangential hyperbolic fluid, temperature, concentration fluid, MHD, oscillatory flow and porous channel.

Each keyword to start on a new line

ABSTRACT

The aim of this research is to study the effect of temperature and concentration on oscillatory flow under the influence of magneto hydrodynamic (MHD) of a non-Newtonian hyperbolic fluid in a horizontal permeable channel. The problem formulation is non-linear and non-homogeneous partial differential equations. Using the perturbation technique, we solve the momentum equation under the assumptions of long wavelength and very low Reynolds number. After obtaining the solution, we used the " Mathematica 13" program to analyze the results through graphs, and the oscillatory flow and magnetic field were studied on the movement of the fluid, its temperature, and concentration.

MSC..

https://doi.org/ 10.29304/jqcsm.2024.16.21549

1. Introduction

In industrial and physiological processes, the non-Newtonian fluids are acknowledged more than viscous fluids. There are several types of non-Newtonian substances that can be seen in nature such like shampoo, paints, ketchup and blood, the tangent hyperbolic fluid model (which is a non-Newtonian fluid). Presented by Sushila. et al [4]. A study on a non-Newtonian tangential hyperbolic fluid with heat transfer through the availability of a heat source with a permeable channel. The governing flow related to non-Newtonian fluids is very complex and its behavior in permeable media varies depending on the model used. Includes blood circulation through the movement of blood, the passage of food, and urination through and urinary tract. The study of Usman et al [7]. Unsteady flow and heat transfer of hyperbolic tangent fluid in the presence of magnetohydrodynamics on an extended plate. In this article, Zehra et al. [8]. presented the analysis of Poiseuille and Couette flows subject to the tangent hyperbolic fluid model through a porous medium. Kareem et al [2]. presented a study on how heat transfer affects the hydrodynamically oscillating flow of a magnet fluid through a porous material under the influence of temperature and concentration. The perturbation technique is a class of analytical methods for finding approximate solutions to nonlinear equations for which an exact solution cannot be obtained. The solution is expressed as a power series in a small parameter, the

∗Corresponding author: Iman S. Salih Al-Shammaria

Email addresses: eamansad12344@gmail.com

Communicated by 'sub etitor'

first term being the known solution to the solvable problem و Successive terms in the series at higher powers usually become smaller. The series is cut and only the first two chapters are kept, and the known problem is solved and the first-degree disorder is corrected.[3]. The most important subject in fluid kinematics through a channel is the magnetic field which is generated from an electric current. It has encouraged other researchers to write about its uses in a variety of science, including the natural and health science, what happens inside stars during their life cycle and what happens inside the sun, such as the rotation of sunspots, are all applications of electrically directed fluid flow [5]. Singhj [6]. presented a study showing the effect of heat transfer on the magnetohydrodynamic oscillatory flow through a porous medium under the influence of temperature and concentration between parallel plates. Kareem et al [1]. presented study on the effect of electrical conductivity on oscillatory flow through porous channels, in addition to a study of the effect of fluid flow on its temperature. These studies inspire us to present a mathematical model to analyze the effect of temperature and the concentration on the MHD oscillatory flow of a tangent hyperbolic fluid through a uniform permeable channel. To solve the problem, we used the perturbation technique. The effect of the parameters is analyzed and discussed through graphs of velocity, temperature and concentration.

2. Mathematical Formulation

Adopted the effect of a simple electric current on a fluid stream through a horizontal channel with small holes in its wall magnetic field to build a mathematical model that controls the oscillating flow of a tangent hyperbolic fluid. The channel has a width of $2h$, and the upper channel wall is affected by a temperature of T_1, so the fluid concentration is C_1 while the lower channel wall temperature is T_0 and the fluid concentration is C_0. We adopted Cartesian coordinates to study the mathematical model, where x represents the horizontal axis and the vertical axis is y and represents the flow field $(u(y,t),0,0)$, which achieves the continuity equation:

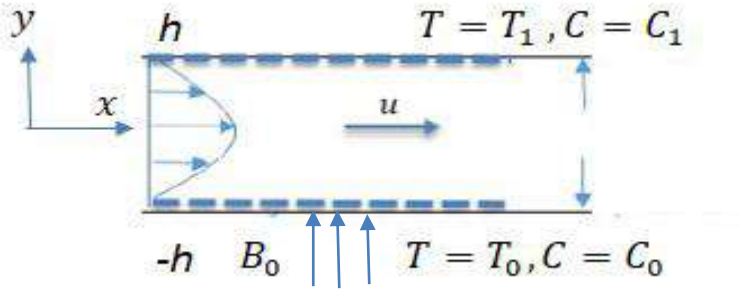

Figure 1: Channel format from [1]**.**

3. Basic Equations:

The basic equations of the system, including the continuity, momentum, temperature and concentration equation, are as: [2]

the continuity equation:

$$\frac{\partial \bar{v}}{\partial \bar{y}} + \frac{\partial \bar{u}}{\partial \bar{x}} = 0. \qquad (1)$$

Momentum equation are:

In the x – direction:

$$\rho\left(\frac{\partial \bar{u}}{\partial \bar{t}} + \bar{u}\frac{\partial \bar{u}}{\partial \bar{x}} + \bar{v}\frac{\partial \bar{u}}{\partial \bar{y}}\right) = -\frac{\partial \bar{p}}{\partial \bar{x}} + \frac{\partial \bar{S}_{\bar{x}\bar{y}}}{\partial \bar{y}} + \rho g \beta_T (T - T_0) + \rho g \beta_C (C - C_1) - \sigma B_0^2 \bar{u} - \frac{\mu_c}{k}\bar{u}. \qquad (2)$$

In the y – direction:

$$\rho\left(\frac{\partial \bar{v}}{\partial \bar{t}}+\bar{u}\frac{\partial \bar{v}}{\partial \bar{x}}+\bar{v}\frac{\partial \bar{v}}{\partial \bar{y}}\right)=-\frac{\partial \bar{p}}{\partial \bar{y}}+\frac{\partial \bar{S}_{\bar{y}\bar{x}}}{\partial \bar{x}}-\sigma B_0^2\bar{v}-\frac{\mu_c}{k}\bar{v}+\rho g\beta_T(T-T_0)+\rho g\beta_C(C-C_1).$$

The temperature equation is given by:

$$c_T\rho(\bar{V}.\nabla)T=K_T\,\nabla^2T+Q_H(T-T_0)-\nabla Q. \tag{3}$$

The concentration equation is given by:

$$(\bar{V}.\nabla)C=D\nabla^2C-K_r^*(C-C_0)+\frac{DK_H}{T_m}\nabla^2T. \tag{4}$$

where $V\equiv(u(y,t),0,0)$ "velocity field", $T(y,t)$ "fluid temperature", $C(y,t)$ is a fluid concentration, , $\bar{S}$ "extra stress tensor" $\bar{p}$ " pressure", μ_c "constant viscosity", ρ "fluid density", B_0 "the field of magnetic strength", k "permeability", c_T "specific heat at constant pressure", K_T "thermal conductivity", Q "radioactive heat flux", Q_H "heat generation" ,D "coefficient of mass diffusivity", K_r^* "chemical reaction coefficient", K_H "thermal diffusion ratio" and T_m "the mean fluid temperature". The conditions for the upper and lower channel walls are given below:

$T=T_1,\mathrm{C}=C_1$ at $\bar{y}=h,$ and $T=T_0,C=C_0$ at $\bar{y}=-h$

The radioactive heat flux [2] is given by:

$$\nabla Q=4\eta^2\,(T_0-T)\,.$$

The fundamental equation for the **tangent hyperbolic** fluid is [7]:

$$\bar{S}\;=[\mu_\infty+(\mu_c+\mu_\infty)\tanh(\Gamma\bar{\dot{\gamma}})^{\mathrm{n}}]\bar{\dot{\gamma}},$$

$$\dot{\gamma}=\sqrt{\frac{1}{2}\sum_i\sum_j\dot{\gamma}_{ij}\dot{\gamma}_{ji}},\;\bar{\gamma}=\nabla\bar{V}+(\nabla\bar{V})^T,$$

where $\overline{\mathrm{V}}=(\bar{u},\bar{v},\bar{w})$ "the velocity field in Cartesian coordinates system (x,y,z)", $\nabla\overline{\mathrm{V}}$ "the gradient of velocity", and $(\nabla\overline{\mathrm{V}})^{\mathrm{T}}$ "the transpose of the velocity gradient".

The stress components are given by:

$$\bar{S}_{\bar{x}\bar{x}}=\bar{S}_{\bar{y}\bar{y}}=0,$$

$$\bar{S}_{\bar{x}\bar{y}}=\bar{S}_{\bar{y}\bar{x}}=\mu_c\left[(1-\mathrm{n})\frac{\partial\bar{u}}{\partial\bar{y}}+\mathrm{n}\Gamma\left(\frac{\partial\bar{u}}{\partial\bar{y}}\right)^2\right], \tag{5}$$

4.Method of Solution:

In order to simplify the governing equations of the problem, we might introduce the following dimensionless transformations as follow [1], [2]:

$$\left.\begin{array}{c}x=\frac{\bar{x}}{h},y=\frac{\bar{y}}{h},u=\frac{\bar{u}}{U},v=\frac{\bar{v}}{U},t=\frac{\bar{t}U}{h},p=\frac{\bar{p}h}{\mu_cU},\Delta T=T_1-T_0,M=\sqrt{\frac{\sigma B_0^2h^2}{\mu_c}},Pe=\frac{c_T\rho hU}{K_T}\\ \theta=\frac{T-T_0}{\Delta T},S_{xy}=\frac{h}{\mu_cU}\bar{S}_{\bar{x}\bar{y}},\Delta C=C_1-C_0,\;\Phi=\frac{C-C_0}{\Delta C},Re=\frac{\rho hU}{\mu_c},We\;=\Gamma\frac{U}{h},Da=\frac{k}{h^2},S_c=\frac{Uh}{D}\\ N=\sqrt{\frac{4\eta^2h^2}{K_T}},E=\frac{h^2Q_H}{K_T},G_c=\frac{\rho g\beta_Ch^2(\Delta C)}{\mu_cU},G_r=\frac{\rho g\beta_Th^2(\Delta T)}{\mu_cU},K_r=\frac{hK_r^*}{U},S_r=\frac{DK_H(T_1-T_0)}{T_mUh(C_1-C_2)}\end{array}\right\} \tag{6}$$

where U "mean flow velocity", Re" Reynolds number", Da "Darcy number", M "magnetic parameter", Pe"Peclet number", N "radiation parameter", We "Weissenberg number", E"the het generation parameter, G_c is solutal Grashof number, G_r is a Grashof number, K_r"the Chemical reaction parameter", S_c"the Schmidt number", and S_r "Soret number".

Substituting equation (6) into equation (1) – (5), we will obtain:

$$\frac{\partial p}{\partial x} = -Re\frac{\partial u}{\partial t} + (1-n)\frac{\partial^2 u}{\partial y^2} + 2nWe\frac{\partial u}{\partial y}\frac{\partial^2 u}{\partial y^2} + G_r\theta + G_c\Phi - \left(M^2 + \frac{1}{Da}\right)u, \quad (7)$$

$$Pe\frac{\partial \theta}{\partial t} = \frac{\partial^2 \theta}{\partial y^2} + (N^2 + E)\theta, \quad (8)$$

$$\frac{\partial \Phi}{\partial t} = \frac{1}{S_c}\frac{\partial^2 \Phi}{\partial y^2} - K_r\Phi + S_r\frac{\partial^2 \theta}{\partial y^2}. \quad (9)$$

Dimensionless boundary conditions for the temperature equation and concentration equation.

$u = 0,\ \theta = \Phi = 1$ at $y = 1$

$u = \theta = \Phi = 0$ at $y = -1$

5. Solution of the Problem:

In this part, the temperature equation and concentration equation are solved, and then the momentum equation.

5.1 Solution of the temperature equation

To solve the temperature equation (8) for the following boundary conditions $\theta(1) = 1, \theta(-1) = 0$.

Let $\theta(y,t) = \theta_0 e^{i\omega t}$ and by substituting into equation (8), after simplifying the result, we obtain:

$$\frac{\partial^2 \theta_0}{\partial y^2} + (N^2 + E - i\omega Pe)\theta_0 = 0. \quad (10)$$

Therefore, the temperature function is:

$$\theta(y,t) = \left(\left(\frac{1}{2}e^{-it\omega}\mathrm{Sec}[\sqrt{A}]\right)\mathrm{Cos}[\sqrt{A}y] + \left(\frac{1}{2}e^{-it\omega}\mathrm{Csc}[\sqrt{A}]\right)\mathrm{Sin}[\sqrt{A}y]\right)e^{i\omega t}. \quad (11)$$

5.2 Solution of the concentration equation

To solve the heat equation (9) for the following boundary conditions $\Phi(1) = 1, \Phi(-1) = 0$.

Let $\Phi(y,t) = \Phi_0 e^{i\omega t}$ and by substituting into equation (9), after simplifying the result, we obtain:

$$\frac{\partial^2 \Phi_0}{\partial y^2} - S_c(K_r + i\omega)\Phi_0 = -S_c S_r\frac{\partial^2 \theta_0}{\partial y^2}. \quad (12)$$

Therefore, the concentration equation is:

$$\Phi(y,t) = e^{i\omega t}\left(e^{\sqrt{B}y}\left(\frac{e^{3\sqrt{B}-it\omega}(A+B+AS_cS_r)}{(A+B)(-1+e^{4\sqrt{B}})}\right) + e^{-\sqrt{B}y}\left(-\frac{e^{\sqrt{B}-it\omega}(A+B+AS_cS_r)}{(A+B)(-1+e^{4\sqrt{B}})}\right) - \frac{Ae^{-it\omega}\mathrm{Csc}[2\sqrt{A}]\mathrm{Sin}[\sqrt{A}(1+y)]S_cS_r}{A+B}\right). \quad (13)$$

5.3 Solution of the momentum equation

To solve the momentum equation with the following boundary conditions,

$\bar{u} = 0$ at $\bar{y} = h$, and $\bar{u} = 0$ at $\bar{y} = -h$. from equation (7) Therefore, dimensionless boundary conditions are:$u(1) = u(-1) = 0$, hence let

$$-\frac{\partial p}{\partial x} = \lambda e^{i\omega t}, \tag{14}$$

$$u(y,t) = u_0(y)e^{i\omega t}, \tag{15}$$

where ω "be an oscillation of frequency" and λ "real constant".

By substituting equation (14)-(15) by equation (7), we have

$$\frac{\partial^2 u_0}{\partial y^2} + \left(\frac{i\omega\, Re + M^2 + \frac{1}{Da}}{n-1}\right) u_0 - \frac{2n}{n-1} We\, e^{i\omega t} \frac{\partial u_0}{\partial y}\frac{\partial^2 u_0}{\partial y^2} = \frac{\lambda + G_T\theta_0 + G_c\Phi_0}{n-1}. \tag{16}$$

with boundary condition $u_0(1) = u_0(-1) = 0$ (17)

Equation (16) we obtained a non-linear differential equation and it is difficult to find the exact solution to it, so we resorted to using the perturbation technique to find a solution to the equation, as follows:

$$u_0 = u_{00} + We u_{01} + 0(We^2). \tag{18}$$

Now, by substituting equation (18) in equation (16), With boundary condition $u_0(1) = u_0(-1) = 0$, we obtain the following results presented in the forthcoming subsections:

I - Zeros-order system (we^0)

$$\frac{\partial^2 u_{00}}{\partial y^2} + \left(\frac{i\omega\, Re + M^2 + \frac{1}{Da}}{n-1}\right) u_{00} = \frac{\lambda + G_T\theta_0 + G_c\Phi_0}{n-1}. \tag{19}$$

The associated boundary conditions $u_{00}(1) = u_{00}(-1) = 0$

II – First- order system (we^1)

$$\frac{\partial^2 u_{01}}{\partial y^2} + \left(\frac{i\omega\, Re + M^2 + \frac{1}{Da}}{n-1}\right) u_{01} = \frac{2n}{n-1}\, e^{i\omega t} \frac{\partial u_{00}}{\partial y}\frac{\partial^2 u_{00}}{\partial y^2}. \tag{20}$$

The associated boundary conditions $u_{01}(1) = u_{01}(-1) = 0$

By substituting the solution of equations (19) and (20) into equations (18), we obtain:

$$u(y,t) = e^{it\omega}\left(\frac{F}{D} - \frac{F\mathrm{Sec}[\sqrt{D}]}{D}\mathrm{Cos}[\sqrt{D}y] + We\left(\left(\frac{e^{it\omega}F^2 n\mathrm{Csc}[\sqrt{D}]\mathrm{Sec}[\sqrt{D}]^2\mathrm{Sin}[2\sqrt{D}]}{3D^{3/2}(-1+n)}\right)\mathrm{Sin}[\sqrt{D}y] - \frac{e^{it\omega}F^2 n\mathrm{Sec}[\sqrt{D}]^2\mathrm{Sin}[2\sqrt{D}y]}{3D^{3/2}(-1+n)}\right)\right). \tag{21}$$

where $B = S_c(K_r + i\omega)$, $A = (N^2 + E - i\omega Pe), D = \left(\frac{i\omega\, Re + M^2 + \frac{1}{Da}}{n-1}\right)$,

and $F = \left(\frac{\lambda + G_T\theta_0 + G_c\Phi_0}{n-1}\right)$.

6. Results and Discussion

In this section, we discuss and analyze graphically the temperature and concentration of the MHD oscillatory flow of a tangent hyperbolic fluid through a bound permeability channel, using the program “Mathematica 13”.

This section is divided into three subsections: the first discusses the effect of parameters on fluid velocity, the second analyzes the effect of parameters on temperature, and the third discusses the effect of parameters on concentration. and all results were graphed in the region $-1 \leq y \leq 1$, which is the diameter of the flow channel.

6.1 Velocity Distribution

The Figures (2)-(17) show the effect of parameters G_T, Kr, t, G_c, λ, Da, Pe, E, Sr, Sc , We, M, ω, N, n and Re respectively, on the distribution of velocity. Figure (2), shows that u increases in the middle of the channel, but it decreases near the channel's walls when increases the parameter G_T. Figure (3), demonstrates how the impact of Kr on velocity profile u diminishes. Figure (4), demonstrates how the impact of (t) on velocity profile u diminishes. As shown in Figure (5), the velocity profile u increases from the middle of the channel to its upper channel wall while it decreases at the lower channel wall when the parameter G_c, increases. We notice in Figure (6), The velocity profile u increases as the parameter λ rise. As see in Figure (7), The velocity profile u increases as the parameter Da rises. Figure (8), illustrates that as the parameter Pe are increased, the velocity profile u decreases in the middle of the channel. Figure (9), shows that u increases in the middle of the channel, but it decreases near the channel's walls when increases the parameter E. Figure (10), illustrates that as the parameter Sr are increased, the velocity profile u decrease. Figure (11) illustrates that as the parameter Sc are increased, the velocity profile u decrease. As shown in Figure (12). We parameter, it increases the fluid velocity near the upper channel wall and vice versa at the lower channel wall, where the fluid velocity decreases with the increase of, W_e parameter. We notice in Figure (13), the parameter M are increased, the velocity profile u decrease. Also, in Figure (14), the velocity profile u decreases in the middle of the channel when the parameter ω increases. Figure (15), shows the increase of the velocity profile in the center of the flow path when the parameter N increases. The velocity profile in the center of the flow path increases when the parameter (n) increases as shown in Figure (16). While in Figure (17), we can observe that as R_e increases, the velocity profile decreases

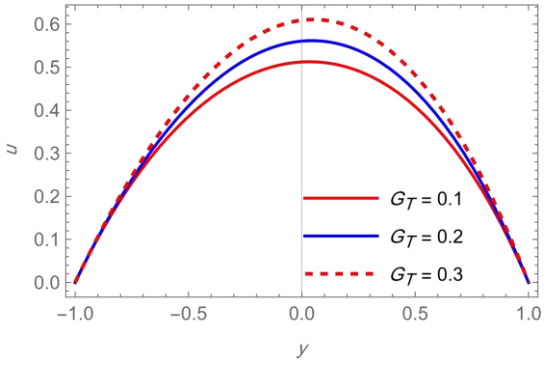

.

Figure 2: Velocity profile with values numbers G_T, with $\omega = 1, N = 1, n = 0.1, R_e = 1, W_e = 0.1, D_a = 0.8, M = 1.2, G_c = 0.1, \lambda = 2, E = 0.8, \mathrm{Pe} = 0.1, K_r = 0.1, S_r = 0.3, S_c = 0.3, i = \sqrt{-1}, t = 0.5$.

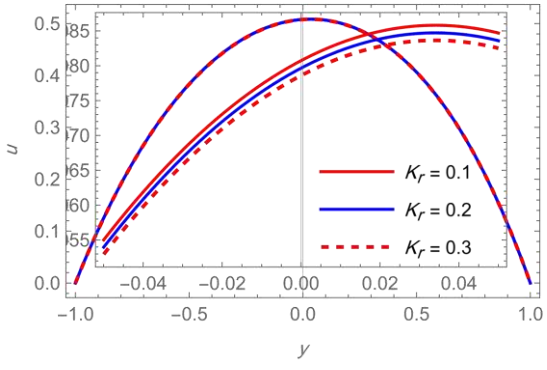

Figure 3: Velocity profile with values numbers K_r, with $G_T = 0.1, \omega = 1, N = 1, n = 0.1, R_e = 1, W_e = 0.1, D_a = 0.8, M = 1.2, G_c = 0.1, \lambda = 2, E = 0.8, \mathrm{Pe} = 0.1, S_r = 0.3, S_c = 0.3, i = \sqrt{-1}, t = 0.5$.

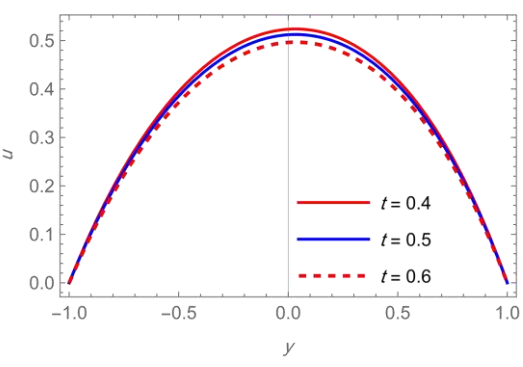

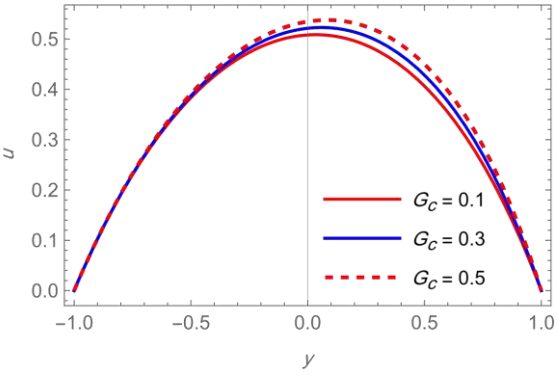

Figure 4: Velocity profile with various coefficients t, with $G_T = 0.1, \omega = 1, N = 1, n = 0.1, R_e = 1, W_e = 0.1, D_a = 0.8, M = 1.2, G_c = 0.1, \lambda = 2, E = 0.8, \mathrm{Pe} = 0.1, K_r = 0.1, S_r = 0.3, S_c = 0.3, i = \sqrt{-1}$.

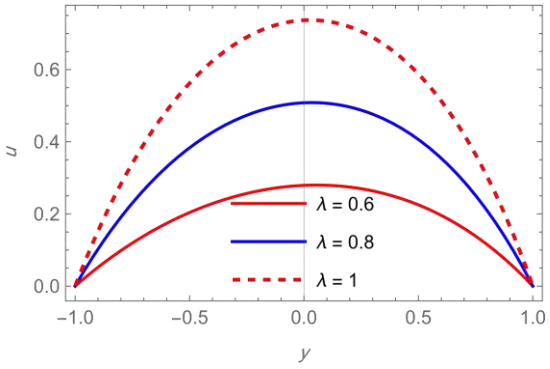

Figure 5: Velocity profile with various coefficients G_c, with $G_T = 0.1, \omega = 1, N = 1, n = 0.1, R_e = 1, W_e = 0.1, D_a = 0.8, M = 1.2, \lambda = 2, E = 0.8, \mathrm{Pe} = 0.1, K_r = 0.1, S_r = 0.3, S_c = 0.3, i = \sqrt{-1}, t = 0.5$.

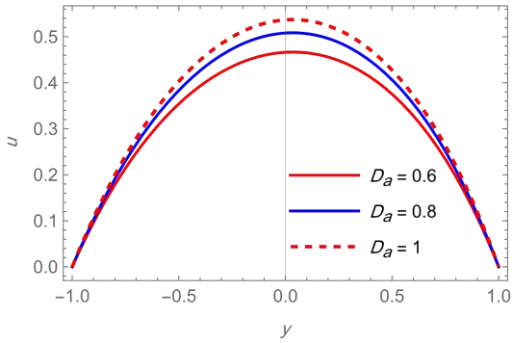

Figure 6: Velocity profile with various coefficients λ with $G_T = 0.1, \omega = 1, N = 1, n = 0.1, R_e = 1, W_e = 0.1, D_a = 0.8, M = 1.2, G_c = 0.1, \lambda = 2, E = 0.8, \mathrm{Pe} = 0.1, K_r = 0.1, S_r = 0.3, S_c = 0.3, i = \sqrt{-1}, t = 0.5$.

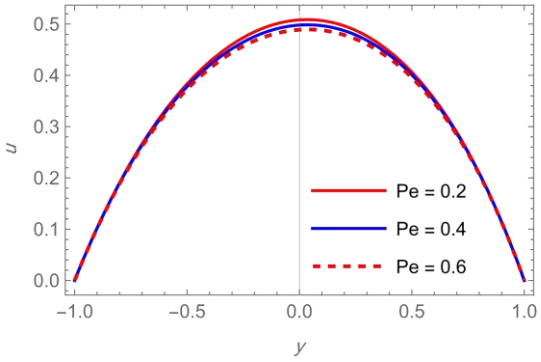

Figure 7: Velocity profile with various coefficients D_a with $G_T = 0.1, \omega = 1, N = 1, n = 0.1, R_e = 1, W_e = 0.1, M = 1.2, G_c = 0.1, \lambda = 2, E = 0.8, \mathrm{Pe} = 0.1, K_r = 0.1, S_r = 0.3, S_c = 0.3, i = \sqrt{-1}, t = 0.5$.

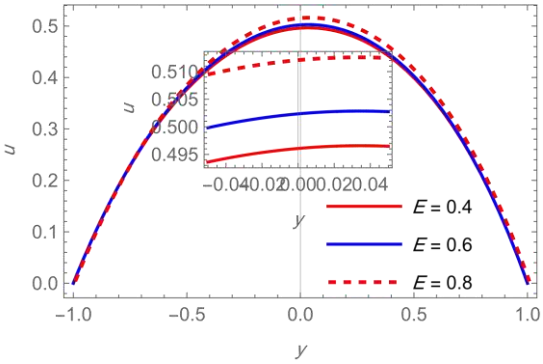

Figure 8: Velocity profile with various coefficients Pe with $G_T = 0.1, \omega = 1, N = 1, n = 0.1, R_e = 1, W_e = 0.1, D_a = 0.8, M = 1.2, G_c = 0.1, \lambda = 2, E = 0.8, K_r = 0.1, S_r = 0.3, S_c = 0.3, i = \sqrt{-1}, t = 0.5$.

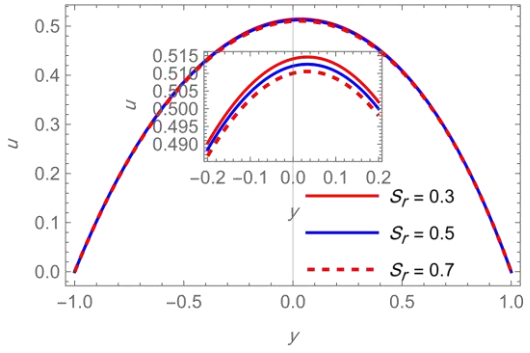

Figure 9: Velocity profile with various coefficients E, with $G_T = 0.1, \omega = 1, N = 1, n = 0.1, R_e = 1, W_e = 0.1, D_a = 0.8, M = 1.2, G_c = 0.1, \lambda = 2, E = 0.8, \mathrm{Pe} = 0.1, K_r = 0.1, S_r = 0.3, S_c = 0.3, i = \sqrt{-1}, t = 0.5$.

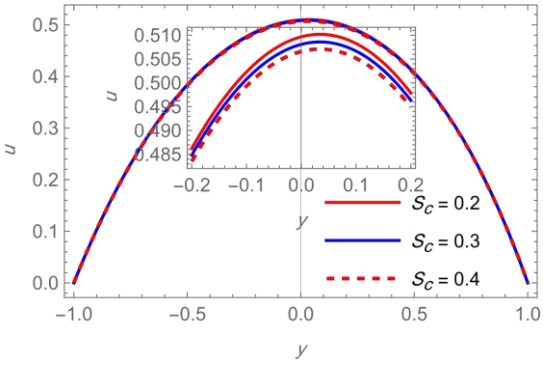

Figure 10: Velocity profile with various coefficients S_r with $G_T = 0.1, \omega = 1, N = 1, n = 0.1, R_e = 1, W_e = 0.1, D_a = 0.8, M = 1.2, G_c = 0.1, \lambda = 2, E = 0.8, \mathrm{Pe} = 0.1, K_r = 0.1, S_c = 0.3, i = \sqrt{-1}, t = 0.5$.

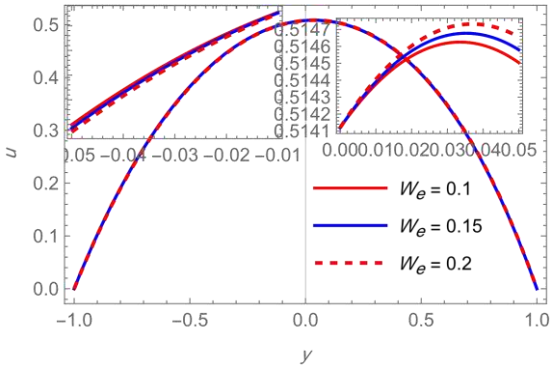

Figure 11: Velocity profile with various coefficients S_c, with $G_T = 0.1, \omega = 1, N = 1, n = 0.1, R_e = 1, W_e = 0.1, D_a = 0.8, M = 1.2, G_c = 0.1, \lambda = 2, E = 0.8, \mathrm{Pe} = 0.1, K_r = 0.1, S_r = 0.3, i = \sqrt{-1}, t = 0.5$.

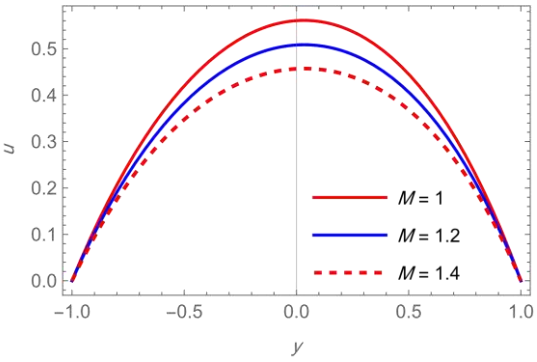

Figure 12: Velocity profile with various coefficients W_e with $G_T = 0.1, \omega = 1, N = 1, n = 0.1, R_e = 1, D_a = 0.8, M = 1.2, G_c = 0.1, \lambda = 2, E = 0.8, \mathrm{Pe} = 0.1, K_r = 0.1, S_r = 0.3, S_c = 0.3, i = \sqrt{-1}, t = 0.5$.

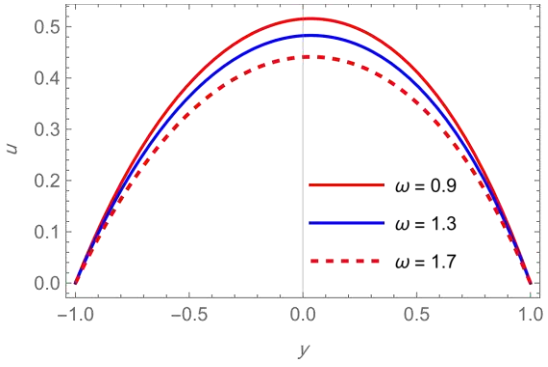

Figure 13: Velocity profile with various coefficients M with $G_T = 0.1, \omega = 1, N = 1, n = 0.1, R_e = 1, W_e = 0.1, D_a = 0.8, G_c = 0.1, \lambda = 2, E = 0.8, \mathrm{Pe} = 0.1, K_r = 0.1, S_r = 0.3, S_c = 0.3, i = \sqrt{-1}, t = 0.5$.

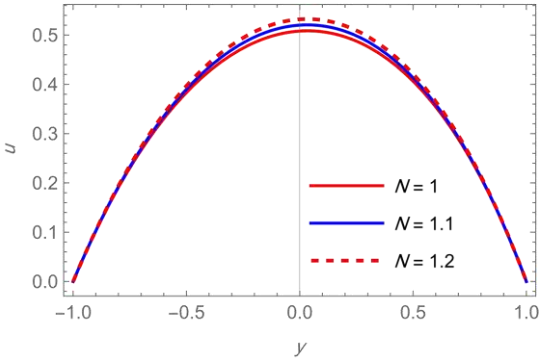

Figure 14 Velocity profile with different values ω, with $G_T = 0.1, N = 1, n = 0.1, R_e = 1, W_e = 0.1, D_a = 0.8, M = 1.2, G_c = 0.1, \lambda = 2, E = 0.8, \mathrm{Pe} = 0.1, K_r = 0.1, S_r = 0.3, S_c = 0.3, i = \sqrt{-1}, t = 0.5$.

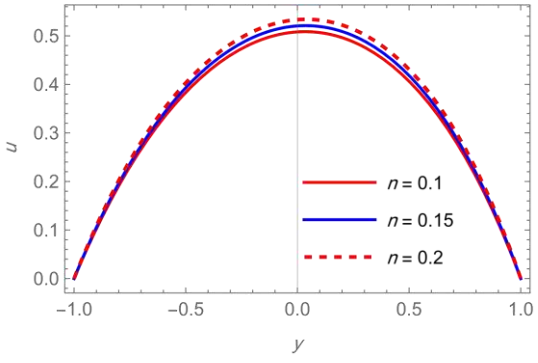

Figure 15 Velocity profile with different values N, with $G_T = 0.1, \omega = 1, n = 0.1, R_e = 1, W_e = 0.1, D_a = 0.8, M = 1.2, G_c = 0.1, \lambda = 2, E = 0.8, \mathrm{Pe} = 0.1, K_r = 0.1, S_r = 0.3, S_c = 0.3, i = \sqrt{-1}, t = 0.5$.

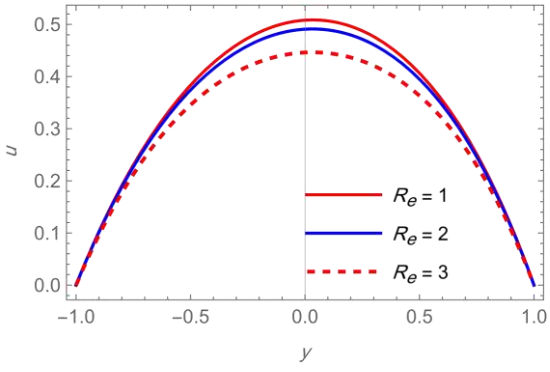

Figure 16 Velocity profile with different values n, with $G_T = 0.1, \omega = 1, N = 1, R_e = 1, W_e = 0.1, D_a = 0.8, M = 1.2, G_c = 0.1, \lambda = 2, E = 0.8, \text{Pe} = 0.1, K_r = 0.1, S_r = 0.3, S_c = 0.3, i = \sqrt{-1}, t = 0.5$.

Figure 17 Velocity profile with different values R_e, with $G_T = 0.1, \omega = 1, N = 1, n = 0.1, W_e = 0.1, D_a = 0.8, M = 1.2, G_c = 0.1, \lambda = 2, E = 0.8, \text{Pe} = 0.1, K_r = 0.1, S_r = 0.3, S_c = 0.3, i = \sqrt{-1}, t = 0.5$.

6.2 Temperature Profile

Figures (18)-(21) show the effect of parameters ω, E, N and Pe on the temperature vs. y. Figure (18),shows that the temperature decreases when parameter ω increases. We can see in Figure (19), that the temperature increases when the parameter E increase. as seen in Figure (20), The temperature rises as N increases. In Figure 21, we can observe that as Pe increases, the temperature lowers

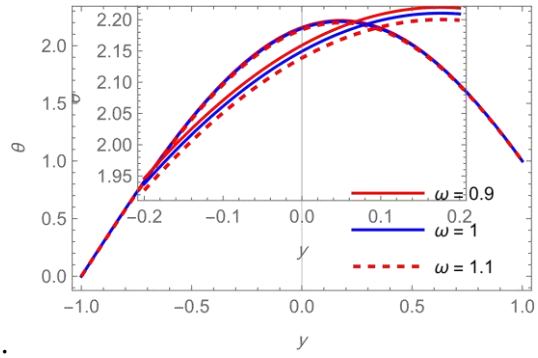

.

Figure18: Temperature profile with different values ω, with $N = 1, n = 0.1, E = 0.8, \text{Pe} = 0.1, i = \sqrt{-1}, t = 0.5$

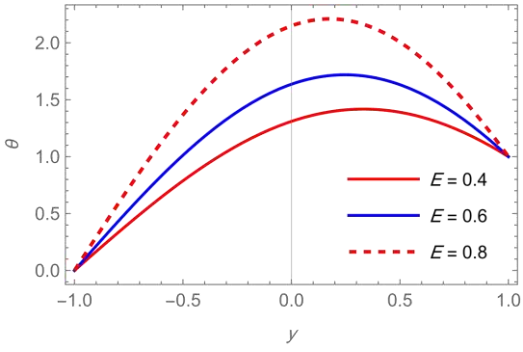

Figure 19: Temperature profile with different values E, with $\omega = 1, N = 1, n = 0.1, \text{Pe} = 0.1, i = \sqrt{-1}, t = 0.5$

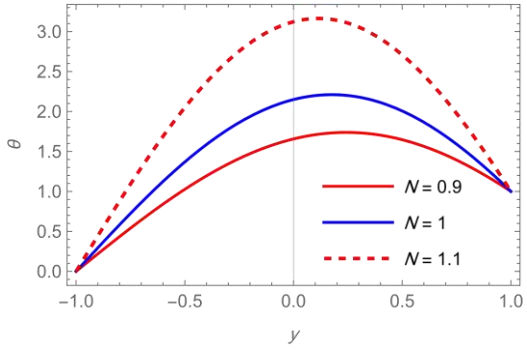

Figure 20: Temperature profile with different values N, with $\omega = 1, N = 1, n = 0.1, E = 0.8, \text{Pe} = 0.1, i = \sqrt{-1}, t = 0.5$

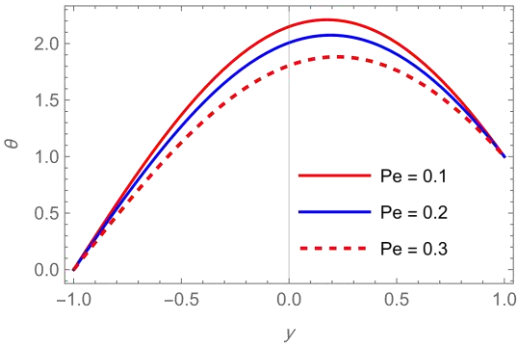

Figure 21: Temperature profile with different values Pe, with $\omega = 1, N = 1, n = 0.1, E = 0.8, i = \sqrt{-1}, t = 0.5$

6.3 Concentration Profile

Figures (22)-(28) show the effect of parameters $E, \omega, \text{Pe}, \text{N}, S_r, S_c$ and K_r on the concentration. Figure (22), shows that when E increases, the concentration decreases. It is evident from Figure (23), that the concentration rises with increasing ω. As shown in Figure (24), the concentration rises with increasing Pe. Figure (25), illustrates how the concentration profile decreases as N rises. How S_r affects the concentration profile decreases is shown in Figure (26). As shown in Figure (27), the concentration Decline with increasing Sc. Figure (28) illustrates how the concentration profile decreases as K_r rises.

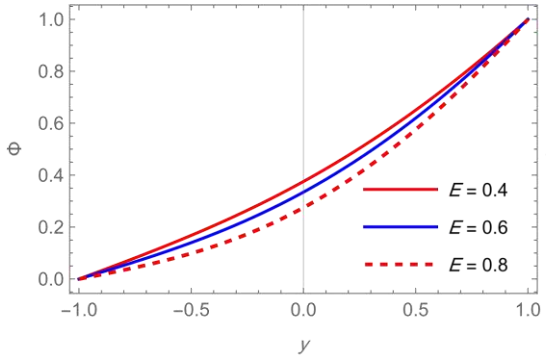

Figure 22: concentration profile with different values E, with $\omega = 1, N = 1, n = 0.1, \mathrm{Pe} = 0.2, K_r = 0.1, S_r = 0.5, S_c = 0.3, i = \sqrt{-1}, t = 0.5$

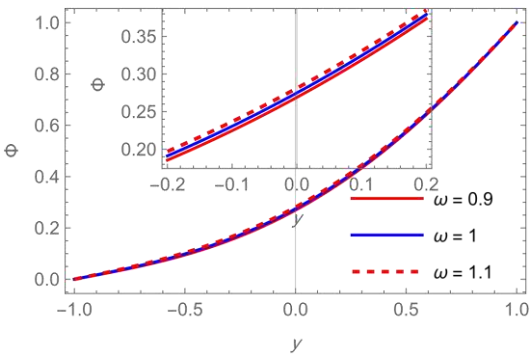

Figure 23: concentration profile with different values ω, with $N = 1, n = 0.1, E = 0.8, \mathrm{Pe} = 0.2, K_r = 0.1, S_r = 0.5, S_c = 0.3, i = \sqrt{-1}, t = 0.5$

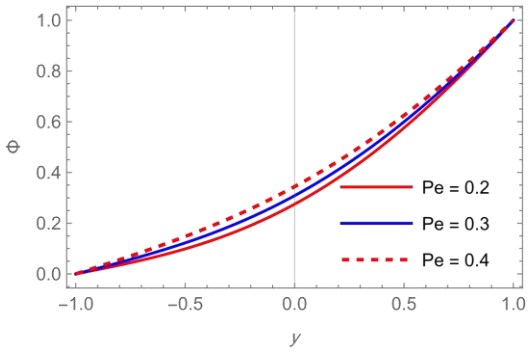

Figure 24: concentration profile with different values Pe, with $\omega = 1, N = 1, n = 0.1, E = 0.8, \mathrm{Pe} = 0.2, K_r = 0.1, S_r = 0.5, S_c = 0.3, i = \sqrt{-1}, t = 0.5$

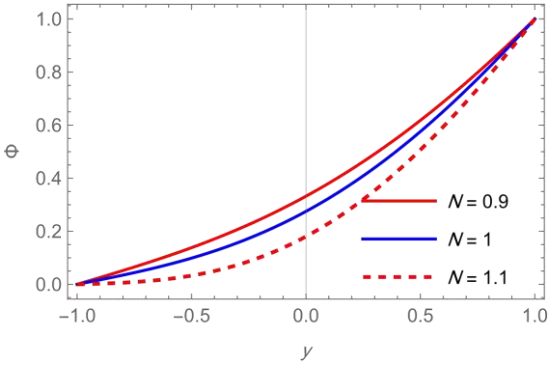

Figure 25: concentration profile with different values N, with $\omega = 1, n = 0.1, Q = 0.8, \mathrm{Pe} = 0.2, K_r = 0.1, S_r = 0.5, S_c = 0.3, i = \sqrt{-1}, t = 0.5$

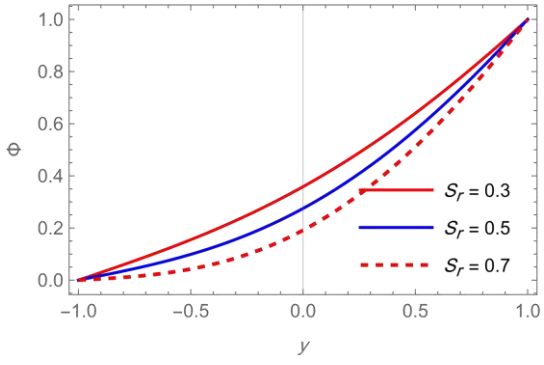

Figure 26: concentration profile with different values S_r, with $\omega = 1, N = 1, n = 0.1, E = 0.8, \mathrm{Pe} = 0.2, K_r = 0.1, S_c = 0.3, i = \sqrt{-1}, t = 0.5$

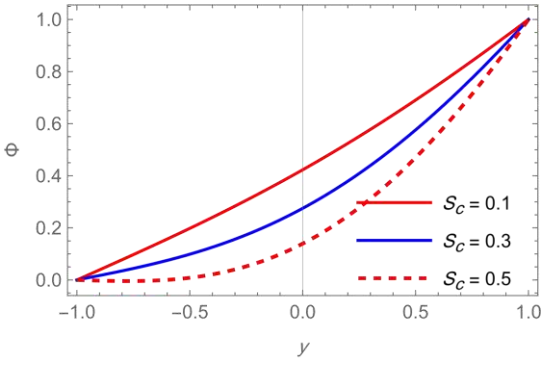

Figure 27: concentration profile with different values S_c, with $\omega = 1, N = 1, n = 0.1, Q = 0.8, \mathrm{Pe} = 0.2, K_r = 0.1, S_r = 0.5, i = \sqrt{-1}, t = 0.5$

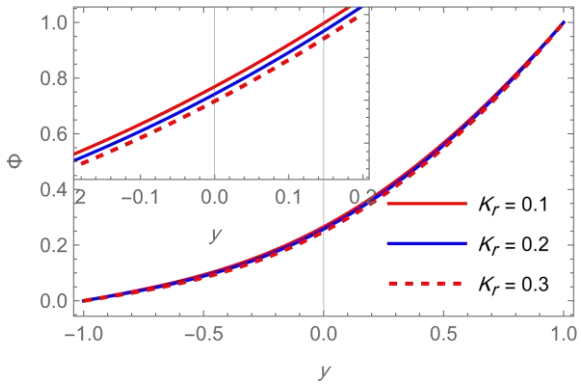

Figure 28: concentration profile with different values K_r, with $\omega = 1, N = 1, n = 0.1, E = 0.8, \mathrm{Pe} = 0.2, S_r = 0.5, S_c = 0.3, i = \sqrt{-1}, t = 0.5$

7- Conclusion Remarks

In this paper, we analyze the temperature, concentration and then study them together on oscillatory flow MHD through a regular horizontal porous channel of a tangential hyperbolic fluid. A summary of the above discussed results is as follows:

- Increasing in the parameters G_r, n, λ, D_a, and G_c leads to fluid's velocity increases, while the fluid's velocity decreases when the following parameters increase M, R_e and t.
- The velocity of the fluid increases in the upper wall of the channel when the parameter We increases, while the effect of the parameter is reflected in the lower wall of the channel and the velocity decreases.
- The parameters E and N have a positive effect on the fluid velocity and temperature, while its effect is negative on the concentration.
- The parameters Sr, Sc and Kr have a negative effect on the fluid velocity and concentration.
- The concentration of the liquid increases and its velocity and temperature decrease when the parameters increase Pe and ω.

References

[1] Al-Kaabi, W. A. M., & Al-Khafajy, D. G. S. (2022, October). Influence of electrical conductivity on the oscillatory flow for Prandtl-Eyring fluid through porous channel. In AIP Conference Proceedings (Vol. 2398, No. 1). AIP Publishing. DOI:10.1063/5.0098173

[2] Al-Khafajy, D. G. S., & Al-Kaabi, W. A. M. (2021). Radiation and mass transfer effects on inclined MHD oscillatory flow for Prandtl-Eyring fluid through a porous channel. Al-Qadisiyah Journal of Pure Science, 26(4), 347-363. DOI: https://doi.org/10.29350/qjps.2021.26.4.1397

[3] Bender, C. M., & Orszag, S. A. (2013). Advanced mathematical methods for scientists and engineers I: Asymptotic methods and perturbation theory. Springer Science & Business Media.

[4] Choudhary, S., Choudhary, P., & Pattanaik, B. (2023). Tangent hyperbolic fluid flow under condition of divergent channel in the presence of porous medium with suction/blowing and heat source: Emergence of the boundary layer. International Journal of Mathematics and Mathematical Sciences, 2023(1), 6282130. DOI:10.1155/2023/6282130

[5] Keith Sharp, M., Carare, R. O., & Martin, B. A. (2019). Dispersion in porous media in oscillatory flow between flat plates: applications to intrathecal, periarterial and paraarterial solute transport in the central nervous system. Fluids and Barriers of the CNS, 16, 1-17. DOI: 10.1186/s12987-019-0132-y

[6] Nigam, S. D., & Singh, S. N. (1960). Heat transfer by laminar flow between parallel plates under the action of transverse magnetic field. The Quarterly Journal of Mechanics and Applied Mathematics, 13(1), 85-97. https://doi.org/10.1093/qjmam/13.1.85

[7] Usman, M., Zubair, T., Hamid, M., Haq, R. U., & Khan, Z. H. (2021). Unsteady flow and heat transfer of tangent-hyperbolic fluid: Legendre wavelet-based analysis. Heat Transfer, 50(4), 3079-3093. https://doi.org/10.1002/htj.22019

[8] Zehra, I., Kousar, N., & Rehman, K. U. (2019). Pressure dependent viscosity subject to Poiseuille and Couette flows via Tangent hyperbolic model. Physica A: Statistical Mechanics and its Applications, 527, 121332. https://doi.org/10.1016/j.physa.2019.121332